Accurate control of optoelectronic amplitude to phase noise conversion in photodetection of ultra-fast optical pulses

Romain Bouchand, Daniele Nicolodi, Xiaopeng Xie, Christophe Alexandre, Yann Le Coq

Research Article | Vol. 25, No. 11 | 29 May 2017 | OPTICS EXPRESS 12268
Optics EXPRESS

Accurate control of optoelectronic amplitude to phase noise conversion in photodetection of ultra-fast optical pulses

ROMAIN BOUCHAND,[1] DANIELE NICOLODI,[1,3] XIAOPENG XIE,[1] CHRISTOPHE ALEXANDRE,[2] AND YANN LE COQ[1,*]

[1] *LNE-SYRTE, Observatoire de Paris, PSL Research University, Sorbonne Universités, UPMC Univ. Paris 06, 61 avenue de l'Observatoire, 75014, Paris, France*
[2] *CNAM, CEDRIC Laboratory, 292 rue Saint Martin, 75003, Paris, France*
[3] *Currently with the National Institute of Standards and Technology, Boulder, Colorado 80305, USA*
[*] *yann.lecoq@obspm.fr*

Abstract: When illuminating a photodiode with modulated laser light, optical intensity fluctuations of the incident beam are converted into phase fluctuations of the output electrical signal. This amplitude to phase noise conversion (APC) thus imposes a stringent constraint on the relative intensity noise (RIN) of the laser carrier when dealing with ultra-low phase noise microwave generation. Although the APC vanishes under certain conditions, it exhibits random fluctuations preventing efficient long-term passive stabilization schemes. In this paper, we present a digital coherent modulation-demodulation system for automatic measurement and control of the APC of a photodetector. The system is demonstrated in the detection of ultra-short optical pulses with an InGaAs photodetector and enables stable generation of ultra-low phase noise microwave signals with RIN rejection beyond 50 dB. This simple system can be used in various optoelectronic schemes, making photodetection virtually insensitive to the RIN of the lasers. We utilize this system to investigate the impact of the radiofrequency (RF) transmission line at the output of the photodetector on the APC coefficient that can affect the accuracy of the measurement in certain cases.

OCIS codes: (320.7090) Ultrafast lasers; (120.5050) Phase measurement; (060.5625) Radio frequency photonics; (120.3940) Metrology.

References and links

1. C. Lisdat, G. Grosche, N. Quintin, C. Shi, S. Raupach, C. Grebing, D. Nicolodi, F. Stefani, A. Al-Masoudi, S. Dörscher, S. Häfner, J.-L. Robyr, N. Chiodo, S. Bilicki, E. Bookjans, A. Koczwara, S. Koke, A. Kohl, F. Wiotte, F. Meynadier, E. Camisard, M. Abgrall, M. Lours, T. Legero, H. Schnatz, U. Sterr, H. Denker, C. Chardonnet, Y. Le Coq, G. Santarelli, A. Amy-Klein, R. Le Targat, J. Lodewyck, O. Lopez, and P.-E. Pottie, "A clock network for geodesy and fundamental science," Nat. Commun. **7**, 12443 (2016).
2. C. Wade, N. Šibalić, N. de Melo, J. Kondo, C. Adams, and K. Weatherill, "Real-time near-field terahertz imaging with atomic optical fluorescence," Nat. Photonics **11**, 40–43 (2017).
3. J. Capmany and D. Novak, "Microwave photonics combines two worlds," Nat. Photonics **1**, 319–330 (2007).
4. P. Ghelfi, F. Laghezza, F. Scotti, G. Serafino, A. Capria, S. Pinna, D. Onori, C. Porzi, M. Scaffardi, A. Malacarne, V. Vercesi, E. Lazzeri, F. Berizzi, and A. Bogoni, "A fully photonics-based coherent radar system," Nature **507**, 341–345 (2014).
5. M. Xin, K. Şafak, M. Y. Peng, A. Kalaydzhyan, P. T. Callahan, W. Wang, O. D. Mücke, and F. X. Kärtner, "Breaking the femtosecond barrier in multi-kilometer timing synchronization systems," IEEE J. Select. Topics Quantum Electron. **23**, 1–12 (2017).
6. K. Şafak, M. Xin, P. Callahan, M. Peng, and F. Kärtner, "All fiber-coupled, long-term stable timing distribution for free-electron lasers with few-femtosecond jitter," Struct. Dyn. **2**, 041715 (2015).
7. X. Xie, R. Bouchand, D. Nicolodi, M. Giunta, W. Hänsel, M. Lezius, A. Joshi, S. Datta, C. Alexandre, M. Lours, P.-A. Tremblin, G. Santarelli, R. Holzwarth, and Y. Le Coq, "Photonic microwave signals with zeptosecond-level absolute timing noise," Nat. Photonics **11**, 44–47 (2017).
8. P.-L. Liu, K. J. Williams, M. Y. Frankel, and R. D. Esman, "Saturation characteristics of fast photodetectors," IEEE Trans. Microw. Theory Techn. **47**, 1297–1303 (1999).
9. M. Currie and I. Vurgaftman, "Microwave phase retardation in saturated ingaas photodetectors," IEEE Photon. Technol. Lett. **18**, 1433–1435 (2006).

#291639 https://doi.org/10.1364/OE.25.012268
Journal © 2017 Received 29 Mar 2017; revised 6 May 2017; accepted 6 May 2017; published 16 May 2017

Optics EXPRESS

10. J. Taylor, S. Datta, A. Hati, C. Nelson, F. Quinlan, A. Joshi, and S. Diddams, "Characterization of power-to-phase conversion in high-speed p-i-n photodiodes," IEEE Photon. J. **3**, 140–151 (2011).
11. W. Zhang, T. Li, M. Lours, S. Seidelin, G. Santarelli, and Y. Le Coq, "Amplitude to phase conversion of ingaas pin photo-diodes for femtosecond lasers microwave signal generation," Appl. Phys. B **106**, 301–308 (2012).
12. T. Fortier, F. Quinlan, A. Hati, C. Nelson, J. Taylor, Y. Fu, J. Campbell, and S. Diddams, "Photonic microwave generation with high-power photodiodes," Opt. Lett. **38**, 1712–1714 (2013).
13. F. N. Baynes, F. Quinlan, T. M. Fortier, Q. Zhou, A. Beling, J. C. Campbell, and S. A. Diddams, "Attosecond timing in optical-to-electrical conversion," Optica **2**, 141–146 (2015).
14. M. Lessing, H. S. Margolis, C. T. A. Brown, P. Gill, and G. Marra, "Suppression of amplitude-to-phase noise conversion in balanced optical-microwave phase detectors," Opt. Express **21**, 27057–27062 (2013).
15. A. Kalaydzhyan, M. Peng, and F. Kartner, "Ultrahigh precision synchronization of optical and microwave frequency sources," J. Phys: Conf. Ser. **741**, 012084 (2016).
16. M. Y. Peng, A. Kalaydzhyan, and F. X. Kärtner, "Balanced optical-microwave phase detector for sub-femtosecond optical-rf synchronization," Opt. Express **22**, 27102–27111 (2014).
17. W. Zhang, S. Seidelin, A. Joshi, S. Datta, G. Santarelli, and Y. Le Coq, "Dual photo-detector system for low phase noise microwave generation with femtosecond lasers," Opt. Lett. **39**, 1204–1207 (2014).
18. A. Haboucha, W. Zhang, T. Li, M. Lours, A. Luiten, Y. Le Coq, and G. Santarelli, "Optical-fiber pulse rate multiplier for ultra-low phase-noise signal generation," Opt. Lett. **36**, 3654 (2011).
19. D. Kuhl, F. Hieronymi, E. H. Bottcher, T. Wolf, D. Bimberg, J. Kuhl, and M. Klingenstein, "Influence of space charges on the impulse response of ingaas metal-semiconductor-metal photodetectors," J. Lightwave Technol. **10**, 753–759 (1992).
20. C.-K. Sun, I.-H. Tan, and J. E. Bowers, "Ultrafast transport dynamics of pin photodetectors under high-power illumination," IEEE Photon. Technol. Lett. **10**, 135–137 (1998).
21. D. Eliyahu, D. Seidel, and L. Maleki, "Rf amplitude and phase-noise reduction of an optical link and an opto-electronic oscillator," IEEE Trans. Microw. Theory Techn. **56**, 449–456 (2008).
22. Z. Abdallah, A. Rumeau, A. Fernandez, G. Cibiel, and O. Llopis, "Nonlinear equivalent-circuit modeling of a fast photodiode," IEEE Photon. Technol. Lett. **26**, 1041–1135 (2014).
23. E. N. Ivanov, S. A. Diddams, and L. Hollberg, "Study of the excess noise associated with demodulation of ultra-short infrared pulses," IEEE Trans. Ultrason., Ferroelect., Freq. Contr. **52**, 1068–1074 (2005).
24. X. Xie, J. Zang, A. Beling, and J. Campbell, "Characterization of amplitude noise to phase noise conversion in charge-compensated modified uni-travelling carrier photodiodes," J. Lightwave Technol. **35**(9), 1718–1724 (2017).
25. E. N. Ivanov, J. J. McFerran, S. A. Diddams, and L. Hollberg, "Noise properties of microwave signals synthesized with femtosecond lasers," IEEE Trans. Ultrason., Ferroelect., Freq. Contr. **54**, 736–745 (2007).
26. K. Wu, P. P. Shum, S. Aditya, C. Ouyang, J. H. Wong, H. Q. Lam, and K. E. K. Lee, "Characterization of the excess noise conversion from optical relative intensity noise in the photodetection of mode-locked lasers for microwave signal synthesis," J. Lightwave Technol. **29**, 3622–3631 (2011).
27. J. Millo, R. Boudot, M. Lours, P. Bourgeois, A. Luiten, Y. L. Coq, Y. Kersalé, and G. Santarelli, "Ultra-low-noise microwave extraction from fiber-based optical frequency comb," Opt. Lett. **34**, 3707–3709 (2009).
28. W. Zhang, M. Lours, M. Fischer, R. Holzwarth, G. Santarelli, and Y. L. Coq, "Characterizing a fiber-based frequency comb with electro-optic modulator," IEEE Trans. Ultrason., Ferroelect., Freq. Contr. **59**, 432–438 (2012).
29. D.-H. Phung and M. Lintz, "Comments on "frequency response of the noise conversion from relative intensity noise to phase noise in the photodetection of an optical pulse train"," IEEE Photon. Technol. Lett. **26**, 1994–1995 (2014).
30. X. Xie, R. Bouchand, D. Nicolodi, M. Lours, C. Alexandre, and Y. Le Coq, "Phase noise characterization of sub-hertz linewidth lasers via digital cross correlation," Opt. Lett. **42**, 1217–1220 (2017).
31. D.-H. Phung, M. Merzougui, C. Alexandre, and M. Lintz, "Phase measurement of a microwave optical modulation: Characterisation and reduction of amplitude-to-phase conversion in 1.5 μm high bandwidth photodiodes," J. Lightwave Technol. **32**, 3759–3767 (2014).
32. W. Zhang, Z. Xu, M. Lours, R. Boudot, Y. Kersalé, G. Santarelli, and Y. Le Coq, "Sub-100 attoseconds stability optics to microwave synchronization," Appl. Phys. Lett. **96**, 211105 (2010).
33. J. Kim and Y. Song, "Ultralow-noise mode-locked fiber lasers and frequency combs: principles, status, and applications," Adv. Opt. Photonics **8**, 465–540 (2016).
34. K. Jung and J. Kim, "Subfemtosecond synchronization of microwave oscillators with mode-locked er-fiber lasers," Opt. Lett. **37**, 2958–2960 (2012).

1. Introduction

Modern photonics commonly relies on low-noise opto-electronics phase transfer through fast photodetection [1–4]. This usually consists in using a fast photodiode to detect a modulated optical carrier and converting it to an electrical signal. The synchronization of optical to microwave signals is fundamental in many applications like long-range timing synchronization, pulse-Doppler radar systems, optical clocks comparison and high stability free-electron lasers [5, 6].

Optics EXPRESS

In particular, unparalleled level of microwave purity can be achieved through synchronization of the repetition rate of an optical frequency comb to a high finesse Fabry-Pérot cavity [7]. In these techniques the fractional frequency stability of an optical reference is transferred to a high-frequency electrical carrier *via* photodetection of the train of narrow optical pulses emitted by an optical frequency comb.

When photodetecting a train of ultrafast optical pulses, the peak optical power is far greater than for continuous wave illumination and the saturation effects that are rapidly appearing in photodetectors are inevitably accompanied by phase distorsion of the RF electrical signal [8, 9]. As a consequence any baseband amplitude noise of the laser light can be up-converted around the RF carrier, hereby disturbing optoelectronic phase transfer through the phenomenon usually called amplitude to phase conversion (APC). The conversion of amplitude noise to phase noise during photodetection is the major obstacle limiting the quality of ultra-low noise optoelectronics phase transfer. It has been found that when saturating a photodetector, for specific operational conditions such as bias voltage and temperature, it exists some optical peak power at which the noise conversion disappears [10, 11]. Sub-femtosecond optical-to-RF synchronization was achieved by operating one photodetector near one of those 'null-APC' points in a direct photodetection (DP) scheme [12, 13] or alternatively by using methods less sensitive to APC like balanced optical-to-microwave phase detector (BOM-PD) [14, 15]. However, unlike BOM-PD, DP suffers from a rapid variation of the coefficient around the APC zero-crossing [16] rendering the quality of the synchronization very dependent on the operational parameters of the photodetector (temperature, bias voltage) and on optical pulse energy. In particular, good levels of APC rejection can only be preserved if the average optical power exhibits fluctuations below the percent level, a value that is beyond many common commercial mode-locked lasers. Otherwise, the performance of photonic microwave generation techniques is then greatly limited or requiring delicate microwave interferometric schemes [17].

In this paper, we overcome this problem and present a simple, relatively low-cost and flexible automatic system for actively stabilizing DP at a state where the APC is nulled. It consists of three key components: an accurate computer-controlled variable fibre optic attenuator, an accousto-optic modulator (AOM) and a software-defined radio (SDR) platform. The setup is calibrated and used to fully characterize the APC of a fast InGaAs photodiode when detecting the repetition rate of an Erbium-doped fibre-based optical frequency comb (scheme similar to [7]). The system we demonstrate allows characterization of the APC coefficient of a photodetector as a function of operational parameters and allows to rapidly find its null-APC points. Laser intensity modulation and coherent demodulation of the phase of the microwave signal provides high sensitivity that allows to measure the APC coefficient for a specific operational parameter in about 5 seconds of integration. This represents a large improvement over previously published that require up to an hour of integration to obtain equivalent uncertainties on the APC coefficient [11, 12]. We use this convenient measurement tool to investigate the APC coefficient biases that can be introduced in the RF transmission line at the output of the photodetector, which has been overlooked in the literature up to now. Finally, we show that without active stabilization the APC coefficient fluctuations prevent from rejecting the RIN by more than approximately 40 dB whereas when using our system to actively stabilize the photodetector near a null-APC point, long-term steady rejection of APC by more than 50 dB is easily achievable.

2. Amplitude to phase noise conversion

2.1. Photodetector saturation

The typical response of an InGaAs photodetector detecting fast femtosecond optical pulses is depicted in Fig. 1. By looking at the RF response at 12 GHz (for a 4 GHz effective pulse repetition rate [18]) shown in Fig. 1 (left panel), one can distinguish three zones corresponding to three different behaviours of the photodetector. Let consider the case for which the applied bias

Optics EXPRESS

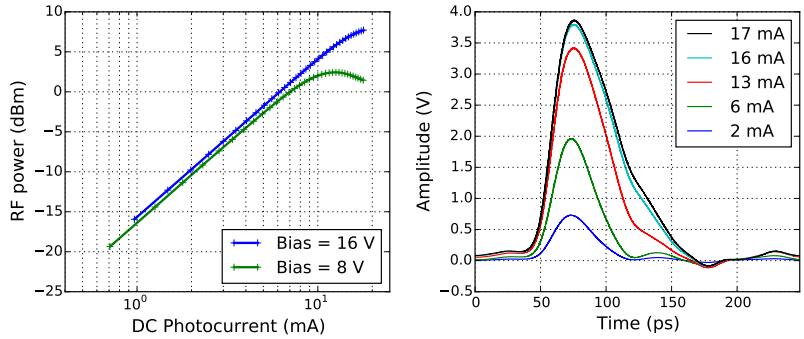

Fig. 1. Power of the 12 GHz harmonics (Left panel) and electrical response (Right panel) obtained after the photodiode under test when detecting the modulated light of an optical frequency comb (4 GHz repetition rate). The electrical responses are measured when the bias voltage is 8 V.

voltage is of 8 V (green line). For small photocurrents up to 5 mA, the RF power is proportional to the square of the photocurrent and the photodiodes is in its linear regime. Between 5 mA and 12 mA the slope of the microwave responsivity decreases until reaching a plateau, this is the saturation regime (sometimes referred to as 'RF saturation'). This arises due to the increase of the electron-hole density in the depletion region whose separation produces an electrical potential opposed to the bias field. This counter-field gradually screens the external bias field up to the point that an increasing optical power is not followed by additional currents, be it DC or RF (this is called the space-charge-screening effect [19, 20]). Above the saturation level, due essentially to the increasing carrier transit time, the photodetector microwave response is lowered when illuminated by higher optical power [21, 22]. This behaviour transpires in the electrical time response (Fig. 1, right panel): when increasing the optical power, the peak voltage starts by increasing without pulse shape distorsion till the inset of saturation when peak voltage remains constant and pulse duration increases causing pulse shape distortion. Thus, in saturation regime, the centroid of the electrical response shifts when the power is varied, causing a power-dependent phase retardation impeding the quality of synchronization between optical and electrical signals. Although the quantitative values of RF power and electrical response depend on the specific characteristics of the photodetector, the qualitative behaviour presented here has been observed in various PIN and modified uni-travelling carrier (MUTC) photodiodes [10–12, 23, 24].

2.2. *Amplitude to phase noise conversion coefficient*

The common way to characterize the fluctuations in the mean optical field of a laser is the relative intensity noise (RIN) while noise on an RF carrier is described in terms of amplitude and phase noise. A measurement of those three quantities when photodetecting the modulated light from a mode-locked laser is reported in Fig.2. The amplitude modulation intentionally introduced, *i.e.* the peak at 1.23 kHz that is present in the optical RIN of the laser, is transferred to the 12 GHz RF carrier obtained after photodetection both as amplitude noise (green line) and phase noise (red line). The 1.23 kHz modulation is then actually up-converted at 12 GHz ± 1.23 kHz. The relative height of the modulation peak in the RIN and in the phase noise clearly indicates that, in this case, photodetection of ultra-fast optical pulses is performed with more than 30 dB of APC rejection. Note that there seems to be a one-to-one correspondence between the baseband RIN of the laser and the amplitude noise of the microwave carrier and this is verified as long as the photodetector is not saturated.

In the context of ultra-low noise photonic microwave generation, the up-conversion of the

Optics EXPRESS

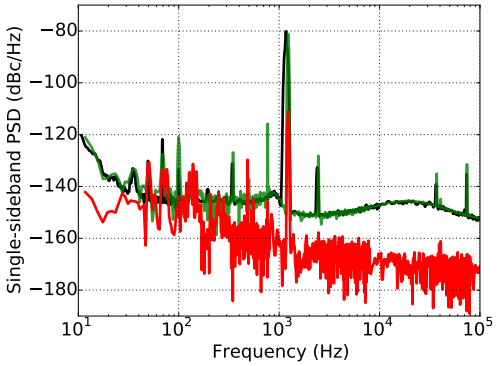

Fig. 2. Optical intensity noise up-conversion. The baseband laser RIN (black line) is transferred to the amplitude noise (green line) and phase noise (red line) of the 12 GHz RF carrier. The noise power spectral densities of the 12 GHz RF carrier are measured using a heterodyne cross-correlation scheme similar to [7]. The laser RIN is measured on a Fast-Fourier-Transform analyser after linear photodetection.

baseband RIN of the laser to the RF carrier is critical as it directly spoils the phase stability of the signal during the transfer from optics to electronics. That is why the understanding and evaluation of the APC in particular keeps drawing the attention. The APC occurring during photodetection is canonically described by a coefficient α describing how the low frequency relative intensity fluctuations of a laser, the RIN $S_I(f)$, are transferred to phase noise of the RF carrier, $S_\phi(f)$:

$$\alpha^2 = \frac{S_\phi(f)}{S_I(f)} \quad [rad^2] \tag{1}$$

where $S_\phi(f)$ and $S_I(f)$ are one-sided double-sideband power spectral densities (PSD) expressed in units of rad^2.Hz^{-1} and Hz^{-1} , respectively. Using the single-sideband definition of phase noise $\mathcal{L}(f)$ commonly used in the photonics industry, the RIN-induced phase noise can be obtained *via* the following formula:

$$\mathcal{L}_{RIN}(f) = 10\ \log[S_I(f)] + \underbrace{20\ \log[\alpha] - 3}_{RINrejection} \quad [dBc/Hz] \tag{2}$$

For commercial InGaAs PIN photodiodes under saturation, α typically ranges from 0.1 to 3.0 radians [10] and similar results were obtained in the case of MUTC photodiodes [12]. However, in previous works the determination of the APC coefficient was rather tedious and not always accurate. In [10], the techniques used by Taylor et al. yield values of the APC coefficient that sometimes agree only by a factor two and do not allow to precisely measure APC coefficient smaller than 0.1 rad. The analogue demodulation methods used by Zhang et al. in [11] are intrinsically slow and every single measurement of the APC coefficient could require up to an hour of integration depending on the level of output signal.

Consequently, given the importance of the APC process contribution to the phase noise of optically generated RF signals, there is still a significant need for a systematic, fast and yet accurate measure of α. In this work we demonstrate a compact and relatively low-cost automatic SDR-based digital demodulation setup for characterizing the APC coefficient. Unlike methods reported previously like *microwave phase bridge* [25], *analogue demodulation* [11] or *impulse response* [26], the digital demodulation method we present is simultaneously simple to set up, reproducible, fast and does not require tedious manual tuning of its parameters. This technique allowed us to study for the first time sources of systematic bias in the APC coefficient

Optics EXPRESS

determination. We verified the measurement accuracy at the ~4 mrad level, limited by the phase fluctuations of the microwave reference used for the phase demodulation.

3. Automatic characterization of amplitude to phase conversion coefficient

3.1. Optical source and photodetector

The 1.5 μm pulsed light source is shown in Fig. 3 (left part) and is based on a fibred optical frequency comb (FOFC) similar to that used in previous works [7]. The typical output light consists of 50 fs optical pulses for a spectrum broader than 60 nm. The repetition rate of the comb (f_{rep} = 250 MHz) is synchronized *via* phase-locking with an ultra-stable laser reference at 1542 nm to achieve fractional frequency stability below 6×10^{-16} at 1 s [27, 28]. It is then increased sixteenfold *via* four cascaded interleavers [18] and the output optical pulses are recompressed by a negative dispersion fibre (DCF38). When impinging on the photodiode, the optical pulses are less than 800 fs long for a repetition rate of 4 GHz and up to 30 mW average optical power. The photodetector under study is a dual-depletion InGaAs PIN photodiode (Discovery Semiconductors, Inc). In our experiment, when it is operated at 8 V reverse bias under 30 mW optical power, it typically yields 2 dBm of 12 GHz microwave power for more than 16 mA DC photocurrent. The photodiode module is not internally terminated so that a bias-tee is used at the output port for 50 Ω termination (cf. Sec. 3.2).

3.2. Setup

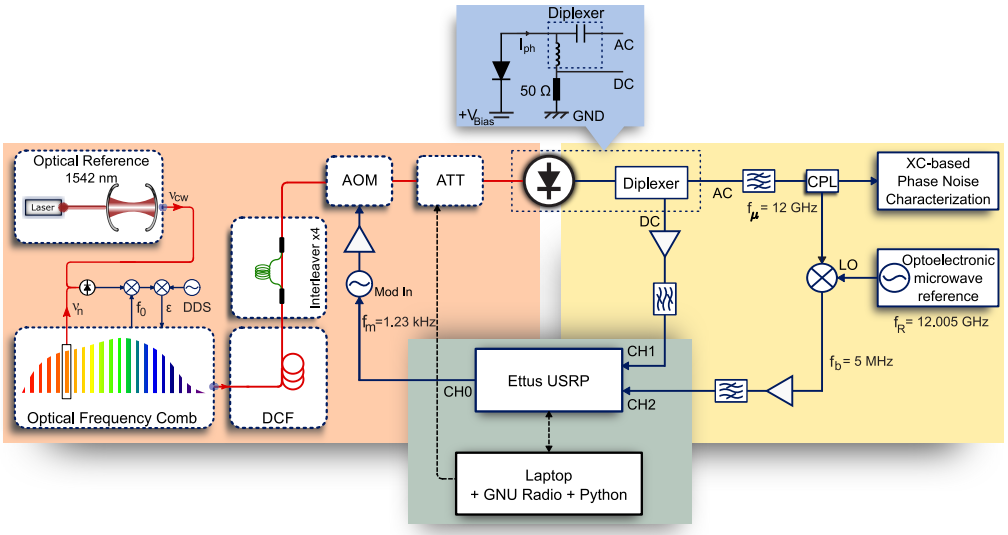

Fig. 3. Setup for the automatic characterization of APC ocurring during the photodetection of a train of ultra-short optical pulses. DCF: dispersion compensation fibre; DDS: direct digital synthesizer; ϵ: error signal; f_0: carrier envelope frequency; ν_n: frequency of the nth comb line; ν_{CW}: frequency of the continuous wave laser reference; GND: ground; V_{Bias}: bias voltage; I_{Ph}: photocurrent; ATT: mechanical fibred optical attenuator; CPL: coupler; XC: cross-correlation; LO: local oscillator; USRP: universal software radio peripheral.

In order to measure the APC coefficient of a photodetector, one needs to measure the phase fluctuations of the photodiode output originating from a known amplitude modulation of the incident optical power. As shown in Fig.3, in our measurement scheme, we perform a modulation (f_m = 1.23 kHz) of the incident light with an AOM (IntraAction Corp.) coupled to the zero order

Optics EXPRESS

and we measure the resulting phase fluctuations on the 12 GHz RF signal after the photodiode using an original heterodyne digital demodulation method *via* a SDR (Universal Software Radio Peripheral N210, Ettus Research). We choose to use an AOM for modulating the amplitude of the laser as modulation of the pump diode current revealed problematic (due mainly to mode-hops of the pump laser diodes and possibly to amplitude to phase coupling arising in the laser itself as stated in [29]). Micro-electro mechanical systems (MEMS)-based light modulator were also tested but they were found to add a substantial amplitude noise. The modulation frequency is chosen to be 1.23 kHz to optimize the amplitude modulation efficiency while keeping away from the power line harmonics.

After passing through a computer-controlled mechanical attenuator (OZ-Optics), the modulated light is directed to the photodiode whose output spectrum consists of harmonics of the repetition rate up to the photodetector roll-off. The output electrical pulses are sent to a broadband diplexer: the DC part (DC-50 MHz) of the photodetected signal is amplified in a low-noise amplifier and fed to a USRP input for digitization (CH1), the AC part (50 MHz-65 GHz) is filtered in a narrow-band (10 MHz) cavity filter to isolate the 12 GHz harmonic which is then sent to a 10 dB microwave coupler. The coupled port output goes in a two-tone termination (T3) triple-balanced mixer (T3-18, Marki Microwave, Inc.) in which it beats with an ultra-stable microwave phase reference derived from another stabilized FOFC. It yields a 5 MHz RF beatnote which is fed to a second USRP input (CH2) for digitization. The output from the coupler transmission port is sent to an optoelectronic cross-correlation system for further phase noise characterization [7, 30]. Careful management of impedance mismatch and electric carrier back-reflections in the mixers proved essential for a sensible determination of the APC coefficient and phase noise measurement. In practice, 40 dB of isolation before each filter and each mixer port, the use of T3 mixers and over 20 dB power difference between the signal driving the LO and the RF ports ensured consistency and repeatability of the results (cf. Sec. 4). The sensitivity of the APC coefficient measurement is limited by the phase noise of the microwave phase reference at the modulation frequency. Although we have performed successfully the phase measurement step with other ultra-low noise sources, the level of RIN rejection we achieve in this work (> 50 dB) requires an extremely low noise microwave phase reference exhibiting phase noise below -130 dBc.Hz^{-1} at 1.23 kHz Fourier frequency, that we obtained from another stabilized FOFC.

3.3. Digital demodulation and APC coefficient computation

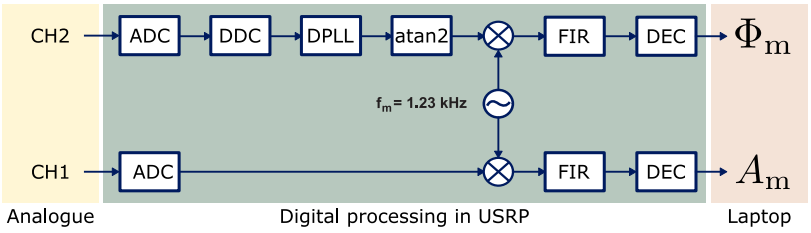

Fig. 4. Simplified block diagram of the digital processing taking place in the USRP for obtaining the amplitude modulation and phase modulation indices. ADC: analogue-to-digital converter; DDC: digital down-converter; DPLL: digital phase lock-loop; atan2: two-argument arctangent function; FIR: finite impulse response filter; DEC: decimation (by 200).

All the control, measurement and actuation is performed with the USRP, the GNU Radio Open-Source software and custom Python code. The USRP generates a sinewave at f_m = 1.23 kHz (CH0) that is used to modulate the 40 MHz drive signal of the AOM while coherently demodulating the relative phase between the 12 GHz microwave signal and the 12.005 GHz ref-

erence oscillator at the same frequency (CH2). It also simultaneously demodulates the amplitude of the DC signal in order to measure the effective amplitude modulation (CH1). As shown in Fig. 4, once fed to the USRP, the input signals are digitized at 100 MS per second to obtain the amplitude and quadrature (IQ) components of the desired modulated signals and down-sampled to 200 kS per second. In the case of the phase demodulation, a digital tracking oscillator is implemented in the software. It locks to the beatnote (whose frequency f_b is close to 5 MHz but not known accurately) and outputs the signal down-converted to DC. The tracking oscillator bandwidth (100 Hz) is kept below the modulation frequency but large enough to provide a satisfying capture range. Then the phase is computed by a two-argument arctangent function and converted back to a complex data stream. At this stage, one has two complex data streams corresponding to an amplitude-modulated signal and to a phase-modulated signal. The next step consists in multiplying the 1.23 kHz modulated complex signals by 1.23 kHz complex sine waves internally generated in the USRP, processing the data through a finite impulse response (FIR) filter and decimating 200-fold. The IQ components corresponding to the output amplitude and phase modulation are saved as two streams of complex numbers (each represented by two 32-bit floats). For each stream the mean IQ phase is calculated and used to compensate for the delay arising between the modulation and demodulation step.

In order to successively probe the photodetector behaviour for different optical powers, a Python-based routine inserted around the GNU Radio code realizes the measurement by several steps, finely tuning the nominal optical power by acting upon the mechanical attenuator (0.01 dB power step resolution). For each step, the phase and amplitude modulation value are averaged for 5 seconds to reach a satisfying measurement resolution and the first second is left out to avoid any transient effects caused by the power change. The APC coefficient can then be derived for each step from the ratio between the phase modulation and the amplitude modulation normalized to the average amplitude: $\alpha = \Phi_m/(A_m/A_{DC})$. We ensured that the APC due to the mixers and amplifiers is negligible using the method described in [31]. Moreover, in order to validate the measurement system, the rejection obtained *via* the USRP is compared with the rejection deduced from a distinct hardware, by comparing the modulation peak in the laser RIN PSD and in the RF phase noise PSD (as was presented in Fig.2).

3.4. Results and discussion

The typical APC coefficient curve obtained is shown in Fig. 5 (top panel). It is expressed as a relative phase change per 100% change in optical power. It depends on the bias applied to the photodiode: increasing the bias voltage pushes the saturation to higher photocurrents. It is consistent with the fact that the reverse field due to the charge screen effect takes a higher density of carrier to collapse the bias field applied (see Sec. 2.1). For a bias voltage of 8 V, the APC coefficient is near-zero (with constant sign) for very low photocurrents, increases monotonically for increasing photocurrents, reaching a maximum of 0.6 radians for a photocurrent of 11 mA and then decreases and crosses zero at roughly 16 mA. Note that when in the saturation regime, the APC coefficient features a sinusoidal behaviour [11, 12] that we cannot see here because of the limited power handling capabilities of the photodiode combined with the high effective repetition rate of the laser (4 GHz).

For 11 mA photocurrent (corresponding to a given optical power and then to a given energy per optical pulse), the value of α means that one percent change in the optical power of the light impinging on the photodiode will shift the phase of the RF carrier under study (12 GHz) by 0.6×10^{-2} radians. In other terms, this implies that for this particular photocurrent, the RIN of the laser is rejected by -7.4 dB (see Eq. eq:rinrejection). The measurements are validated independently by comparing the amplitude of the 1.23 kHz modulation peak in the RIN (obtained with a fast-Fourier transform analyzer) to the amplitude of the corresponding peak in the SSB

Optics EXPRESS

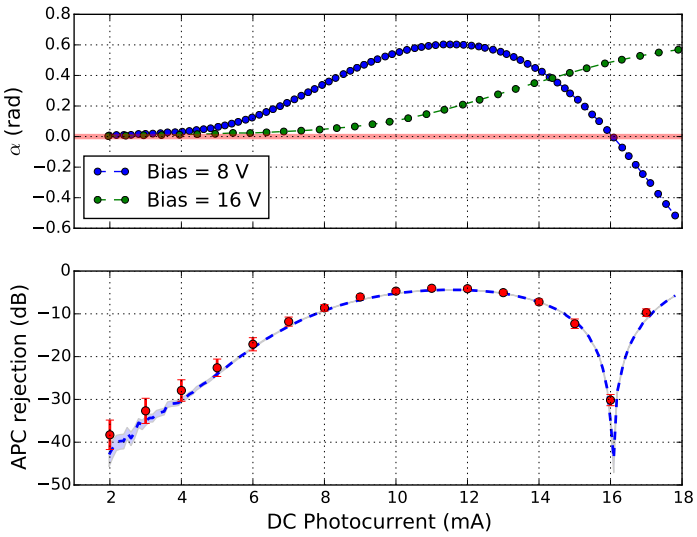

Fig. 5. Top panel: APC coefficient of the photodetector under study for 8 V (blue dots) and 16 V (green dots) bias voltage. It is measured automatically *via* the USRP, each point taking approximately 5 seconds. Bottom panel: APC rejection. The data obtained *via* the USRP system (dotted line) agree well with the rejection inferred from the RIN and the RF carrier phase noise (red dots). The shaded blue area represents the statistical error on the APC coefficient measurement.

power spectral density of phase noise of the 12 GHz carrier obtained *via* optoelectronic cross-correlation (see Fig. 5, bottom panel). The results from the two measurement techniques are in very good agreement, except at small photocurrents (<5 mA), where the small RF power available hinders the microwave phase measurement, making the digital APC coefficient determination not as accurate.

On Fig. 5 (bottom panel, blue line), we observe a zero-crossing at 16 mA photocurrent, for which the phase photodetection process is exactly immune to any amplitude noise of the laser. Indeed it is known that the APC coefficient vanishes for specific optical powers when utilizing photodetectors in a saturated regime [10, 11]. In order to reject the maximum amount of RIN during photodetection, two options arise: either using low fluences for which α remains small or increase the optical power so as to reach full saturation and operate at a null-APC point. Although it could appear attractive to use low photocurrents for which α remains relatively small yet this means reducing the amount of available RF power and raising the levels of Johnson-Nyquist and shot noise signal-to-noise floor limits. The second option is delicate because the positions of these nulls are sensitive to numerous photodetector parameters, including temperature, and vary erratically in time making any passive operation at a null-APC point particularly tedious and limiting its benefit for ultra-low noise photonic microwave generation. However the very fact that the slope is steep around the null makes it particularly suitable for a servo, which is the option we choose in this work.

4. APC coefficient and impedance mismatch

After photodetection of a train of optical pulses from the mode-locked laser, the output of the photodiode consists of electrical pulses the spectrum of which spans typically from DC up to the photodetector bandwidth. In fast photodetectors like the device under test in our experiment, this bandwidth is high (12 GHz) so that special care must be taken in the choice of RF components

Optics EXPRESS

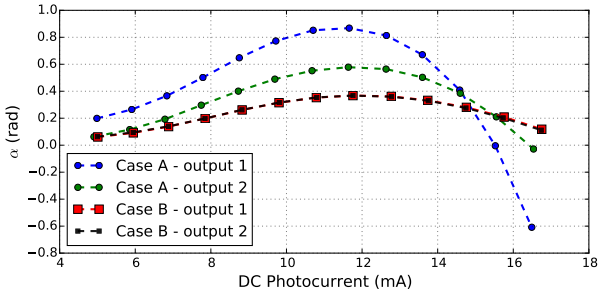

Fig. 6. Impact of isolation and impedance mismatch on the APC coefficient. We measure the APC coefficient at the two different outputs of a coupler when the RF transmission line is improperly isolated (Case A, less than 1 dB of isolation) and properly isolated (Case B, isolation ~ 20 dB). In Case A (circles), there is a significant discrepancy of the APC coefficient obtained at the two coupler outputs while in Case B (squares) the two curves overlap up to the accuracy of the APC coefficient measurement.

to be used directly after the photodiode. Indeed, for such high frequencies the components are seldom broadband and produce reflections disturbing the circuits. On this matter, we report that there are systematic biases in the measurement of α when changing the structure of the RF components in the transmission line between the photodetector and the mixer performing the phase comparison.

Most relevant for the APC active control implemented here, we need to ensure that the APC coefficient measured from a -10 dB fraction of the microwave signal extracted *via* a microwave coupler (see Fig. 3) is the same as the one affecting the main output signal. The potential discrepancy could introduce a bias and lead to a system that locks the APC at a non-zero value. Experimentally, we find that this is only the case when great care is taken regarding impedance mismatch problem in the RF transmission line between the photodiode and the coupler. As an illustration of this remark, we measured the APC coefficient at the output port (output 1) of the coupler and at the coupled port (output 2) for different quality of isolation (see Fig.6). We observe that a lack of proper isolation can introduce biases in the APC coefficient that can go beyond 0.5 rad, leading to shifts in the zero-crossing current by a few milliampere which in our case would defeat the purpose of the APC active control.

Besides this noteworthy phenomenon that can be solved by proper management of the impedance mismatch in the transmission line, we observed a clear influence of the bias-tee used at the output of the photodetector on the APC coefficient. As can be seen in Fig. 7, we measured the APC coefficient for several configuration of the transmission line. We note that when using different bias-tees the APC coefficient changes drastically, in particular the zero crossing shifts by a significant amount. In this measurement, for each bias-tee the isolation in the transmission line is sufficient to avoid the biases mentionned before. We then explain the changes in the APC coefficient by the fact that the bias-tees introduce inevitable delays that further distort the electrical pulses at the output of the photodiode (for instance the group delay is different for 5541A: 213 ps and for SHFDX65: 200 ps). This was verified by measuring the output electrical pulses for different bias-tees as is shown in Fig. 7 (right panel). Similar behaviour was observed when changing the structure of the RF transmission line after the bias-tee, namely: changing the type of isolators, the amount of isolation, changing the place of the filter, adding splitters, couplers or attenuators. The narrower the bandwidth of the component and the closer to the bias-tee, the more drastic its influence on the APC.

The biases observed here are usually not taken into account in the literature and yet can totally spoil the accuracy of the APC coefficient measurement when comparing results obtained with

Optics EXPRESS

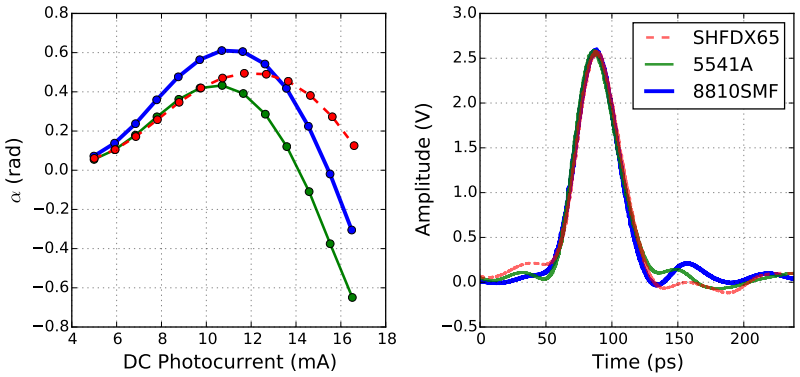

Fig. 7. Left panel: comparison of the APC coefficient characteristics for three different bias-tees (5541A from Picosecond Pulse Labs; 8810SMF from Aeroflex, Inc. and SHFDX65 from SHF Communications Technologies AG) at the output of the photodiode under test. Right panel: electrical pulses obtained after each bias-tee. One can see that the electrical reponse depends on the model of the bias-tee used. Although the peak power remains unchanged, the negative transients in the tail of the response are particularly affected by the choice of bias-tee. Those electrical responses are measured using a sampling oscilloscope clocked by the repetition rate of the optical frequency comb.

different RF components in the transmission line. In particular they could explain the difference in the APC coefficient values obtained with various methods. Eventually, our observations support the fact that during an optoelectronic conversion process the APC coefficient is determined by the ensemble { Photodetector + Coupling to RF + DC loading + RF transmission line }. This confirms partially what was mentioned by Ivanov et al. [23] and differ from the observation by Taylor et al. [10]. In [23], Ivanov et al. explained the dependency of α on the mean optical power purely as a result of the transmission line configuration. We do not fully support this explanation, first because the role of the photodetector has been confirmed elsewhere [21, 26] and second, because the analytical *asymmetric triangular response model* model proposed in [11] gives some insight on the origin of this dependency. However, we do confirm there is an influence of the transmission line after the photodetector on the APC coefficient (unlike what was reported in [10]). The electron dynamics in the junction combined with the coupling circuit seems to be the major reason for causing the APC, hence changes in this dynamics translates as different electrical pulses in the time domain and different APC coefficient in the frequency domain.

5. Active stabilization of amplitude to phase noise conversion

The active stabilization of the photodetection at a null-APC point is achieved through actuation on the mean optical power by feedback on the AOM driving signal, which provides very fine tuning of the power sent to the photodiode. When the stabilization scheme is applied, typical rejection of more than 50 dB of RIN is achievable as can be seen by the 1.23 kHz modulation peak rejection on the residual phase noise measurement shown in Fig. 8 (left panel). It can be maintained for long periods of time.

Note that in the context of photonic microwave generation the level of residual phase noise achieved here is outstanding and comparable with the best reported results [16, 32]. The principal but minute drawback is the small parasitic phase noise introduced through the AOM when modulating the output field of the laser, it consists of a peak at the modulation frequency and its harmonics as well as various spurs between 1 kHz and 10 kHz Fourier frequencies. As this noise is in-loop regarding the APC servo, when operating the photodetector near a null-APC point,

Optics EXPRESS

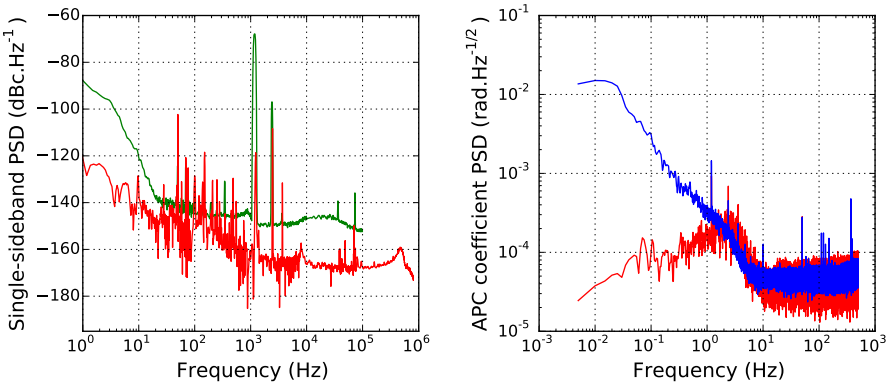

Fig. 8. Left panel: residual 12 GHz microwave carrier phase noise characterized by cross-correlation (red line). The RIN (green line) is shown for appreciating qualitatively the rejection of amplitude to phase noise conversion. Right panel: inloop power spectral density of the APC coefficient with (red line) and without (blue line) the active control.

this noise is significantly reduced. Finally, as some spurious noise comes from the noise of the synthesizer used to drive the AOM (ifr2023A, Aeroflex Inc.) and from the modulation source (digitally synthesized by the Ettus) it is possible to further improve the overall performance by using lower noise RF signal generators.

The inloop power spectral density of α is shown in Fig. 8 (right panel). The free running curve (blue line) indicates that random fluctuations of α are on time scales corresponding typically to Fourier frequencies lower than 7 Hz. Above this Fourier frequency, we can see a plateau at approximately $5 \times 10^{-5}\, rad^2.\mathrm{Hz}^{-1/2}$. We attribute this white noise floor to the phase measurement system, especially to the phase noise of the optoelectronic phase reference used for generating the 5 MHz beatnote on which the phase demodulation is performed. To verify this statement, we observed that when the optoelectronic reference is changed for a lower quality one we see a significant rise of this plateau. This is one of the main limitation of the system, although the phase reference is a stabilized femtosecond laser that exhibits remarkably low phase noise levels. The system described here is of particular interest for state-of-the-art photonic microwave generation with common commercial fibre-based optical frequency combs which typically exhibit -120 dBc.Hz^{-1} or worst relative intensity noise [33] and would thus greatly benefit from the additional rejection provided by the automatic control of APC demonstrated here.

6. Amplitude to phase noise conversion dynamics

Apart from the accurate and stable control of APC during fast photodetection, the automatic system we demonstrate here offers the opportunity to study the dynamics of the APC coefficient over long period of time. As can be seen in Fig. 9 (top panel), when there is no stabilization (blue line) scheme the coefficient is stochastic and fluctuates around the null-APC point up to 11 mrad which means that only 40 dB of APC rejection can be guaranteed. Besides we observe on Fig. 9 (bottom panel) that the two-sample (Allan) overlapping deviation of the APC coefficient decreases with the square root of the integration time up to 50 ms and then drifts as a random walk ($\propto \tau^{1/2}$). This behaviour calls for a stabilization with a bandwidth of about 50 to 100 ms. When the active control is on, the APC coefficient fully adopts a white noise behaviour and the Allan variance is almost totally decreasing as ($\propto \tau^{-1/2}$) apart from a small bump due to the servo itself. Subsequently, when we lock on the null-APC point by acting on the AOM the APC

Optics EXPRESS

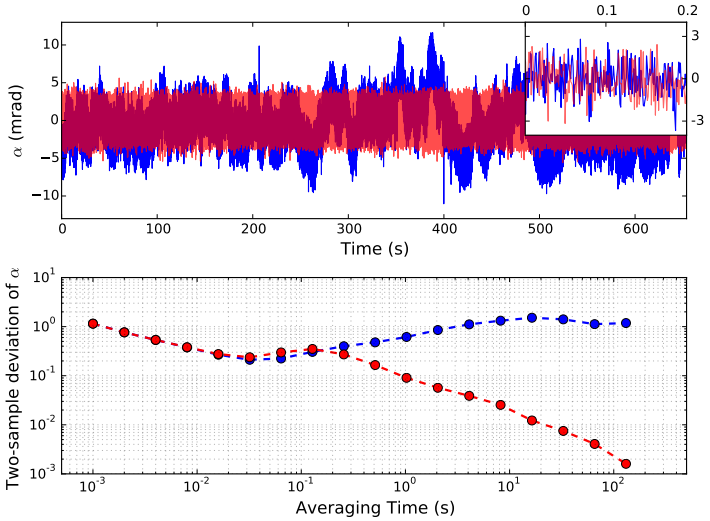

Fig. 9. Top panel: dynamics of the amplitude to phase conversion coefficient without (blue) and with (transparent red) active control over 650 seconds of acquisition. A zoom on a short time scale (0.1 second) is shown in the inset to emphasize that the high frequency behaviour of α is similar for both cases, although it seems the red stream is wider than the blue stream on the long time acquisition (due to the large number of samples and to the graphical linewidth). Bottom panel: overlapping two-sample (*Allan*) deviation of the amplitude to phase coefficient computed over the same acquisitions without (blue) and with (red) active control. The error bars are too small to be represented on this graph.

Table 1. Overview of the RIN rejection and residual phase noise recently reported in the literature in the case of BOM-PD and DP when extracting a microwave signal from an optical frequency comb. Note that in all those works except in the method presented here and in [7], the APC coefficient (and then the RIN rejection) is inferred *a posteriori* from the overall microwave phase noise results.

		RIN rejection	Carrier frequency	Residual phase noise	
				at 1 Hz	at 10 kHz
		dB	GHz	dBc/Hz	dBc/Hz
BOM-PD	(2012) Jung et al. [34]	27	8.06	-133	-154
	(2013) Lessing et al. [14]	63	8	-131	-147
	(2014) Peng et al. [16]	53	10.22	-139	-161
DP	(2013) Fortier et al. [12]	23	10	-112	-162
	(2015) Baynes et al. [13]	44	10	-135	-170
	(2017) Xie et al. [7]	33	12	-107	-173
	This work	51	12	-120	-166

Optics EXPRESS

coefficient is kept steady below the 4 mrad level, hereby ensuring more than 50 dB of laser RIN rejection. This can be verified by the level of residual phase noise on the 12 GHz carrier shown in Fig. 8 (left panel) that constitutes an out-of loop validation of the rejection. In the case of direct microwave extraction from femtosecond lasers, it is the best rejection ever reported to our knowledge (cf. Table. 1), and unlike previous works this level of rejection is repeatable, and stable over long term experiments.

7. Conclusion

We demonstrate the use of an SDR-based scheme for measuring accurately and rapidly the APC coefficient arising during photodetection of a low-jitter train of pulses from an optical frequency comb. It allows to quickly characterize a PIN photodetector and find one of its null-APC point. In particular, we use this system to study the impact of the RF circuit at the output the photodiode on the APC coefficient, which was underestimated so far in other works on the subject. Besides, active stabilization of fast photodetection at a null-APC point is achieved by real-time measurement of the amplitude to phase noise conversion coefficient and tuning of the average optical power through actuation on an AOM coupled to the zero-order. The amplitude to phase conversion lock yields over 50 dB of relative intensity noise rejection for long periods and allows the generation of ultra-low noise 12 GHz microwave carrier with levels of residual phase noise comparable to the best schemes (-120 dBc.Hz^{-1} at 1 Hz Fourier frequency, -165 dBc.Hz^{-1} at 1 kHz and -170 dBc.Hz^{-1} at 30 kHz). In particular, the reproducible setup presented here could offer the opportunity to use compact but high-RIN fibred laser for generating state-of-the-art microwave signals over large time-scales without the need for tedious RIN management. The system could also be improved to allow simultaneous control of multiple photodetection systems at a null-APC point, however as this point is photodetector-dependent, such a scheme would require more channels than available in our current SDR hardware. Finally, in view of the APC biases studied in this work, ingenious choice of the structure of the RF transmission line and loading circuit at the output of the photodetector could reduce the APC coefficient by a significant amount.

Funding

Defense Advanced Research Projects Agency (DARPA) as a part of the Program in Ultrafast Laser Science and Engineering (PμreComb project) under contract no. W31P4Q-14-C-0050; Formation, Innovation, Recherche, Services et Transfert en Temps-Fréquence (FIRST-TF) Labex; Eurostar Eureka program (Stable Microwave Generation and Dissemination over Optical Fiber project - STAMIDOF).

Acknowledgments

We thank J. Pinto for his help with the electronics and M. Lours for his expertise in designing low noise radio-frequency chains.